Catalysis Today 175 (2011) 504–508

Contents lists available at ScienceDirect

Catalysis Today

journal homepage: www.elsevier.com/locate/cattod

On-board H_2 generation by catalytic dehydrogenation of hydrocarbon mixtures or fuels

Carlo Lucarelli[a], Stefania Albonetti[a], Angelo Vaccari[a,*], Carlo Resini[b], Gilles Taillades[b], Jacques Roziere[b], Kan-Ern Liew[c], Alexander Ohnesorge[c], Christian Wolff[c], Ilenia Gabellini[d], David Wails[d]

[a] Dip. di Chimica Industriale e dei Materiali, Alma Mater Studiorum – University of Bologna, Via Risorgimento 4, 40136 Bologna, Italy
[b] ICGM – Aggregates, Interfaces, Materials for Energy, CNRS-University Montpellier 2, France
[c] EADS Deutschland GmbH, Willy-Messerschmitt Strasse, D-81663 Munich, Germany
[d] Johnson Matthey Technology Centre, Sonning Common, Reading, Berkshire RG4 9NH, United Kingdom

ARTICLE INFO

Article history:
Received 14 October 2010
Received in revised form 9 February 2011
Accepted 28 February 2011
Available online 13 April 2011

Keywords:
Hydrogen production
Dehydrogenation
Pt/Sn catalysts
Kerosene surrogate

ABSTRACT

The partial dehydrogenation (PDh) of hydrocarbon blends may be a suitable way to produce H_2 on-board of automotives or airplanes to feed fuel cells and produce electric power, avoiding storage problems. In this work very interesting data have been collected using Jet A-1 surrogate and Pt–Sn/γ-Al_2O_3 catalysts, operating at 450 °C and feeding the vaporised hydrocarbon blend without any carrier gas. The use of Pt/Sn catalyst with 1:1 (w/w) ratio leads to the best compromise between activity and stability with time-on-stream, due to the formation of Pt-rich alloys. Nevertheless, all studied catalysts exhibited limited thio-tolerance. In optimized reaction conditions, H_2 productivity of 3000 NL/kg_{cat}/h, sufficient to produce 3 kW of electric power, considering purification steps and a fuel efficiency of 50%, was obtained.

1. Introduction

To avoid problems of storage and transport, on-board efficient H_2 production technologies are drawing more and more attention [1–5]. The dehydrogenation of cyclic hydrocarbons with high hydrogen content, known also as "chemical hydrides" or "organic hydrides" is a promising method for storing and transporting hydrogen [4,6–8]. Moreover, the idea to use fuels like diesel or kerosene cuts as a H_2 source is attracting increasing interest [9,10], with the goal to further upgrade an already valuable energy carrier (the fossil fuel) by extracting another energy carrier (H_2).

The lack of oxygen in hydrocarbon fuels make them suitable for partial dehydrogenation products which are liquid phase dehydrogenated hydrocarbons and gas phase H_2, easy to separate. Therefore, because of the absence of carbon oxides, the gas stream may be directly fed without any further purification to on-board PEM fuel cells to supply electric energy to auxiliary systems on heavy duty transportation systems, such as ships and aircraft. The liquid mixture, composed of partially dehydrogenated hydrocarbons, still maintains its original fuel properties making hydrocarbon fuels appealing H_2-storage media. Although several different metal-supported catalysts have been investigated for cycloalkane dehydrogenation, Ni and Pt are among the most used metals [4,6,10–14]: Ni is cheaper than Pt, but less selective in dehydrogenation reactions and favours cracking reactions at high temperatures. The support also plays a key role and different types have been investigated, like alumina [6,10,15], alumina-sulfated zirconia [10], silica [17], activated carbon [11,13,16], carbon nanofibres [8,18,19] or nanotubes [14].

The set-up of the catalyst for hydrocarbon fuel dehydrogenation to produce H_2 without compromising the original fuel properties is a key-point; the tailored catalyst has to favour dehydrogenation or reforming (isomerisation, cyclisation, aromatisation) reactions, avoiding polymerisation or cracking reactions, responsible for coke deposition and catalyst deactivation. The open literature is rather poor on this topic, and it appear that only Wang et al. have studied this subject [10]. The aim of the work described below was the preparation and characterisation of alumina supported Pt–Sn catalysts for partial dehydrogenation of Jet A-1 surrogate fuel to produce H_2 to feed on-board PEM fuel cells.

2. Experimental

2.1. Catalyst preparation

Three catalysts, 1 wt.% Pt/γ-Al_2O_3, and 1 wt.%Pt–1 wt.%Sn/γ-Al_2O_3 and 1 wt.%Pt–3 wt.%Sn/γ-Al_2O_3, hereinafter called Cat1, Cat2 and Cat3 respectively (Table 1), have been prepared by two

* Corresponding author. Tel.: +39 051 2093683; fax: +39 051 2093679.
E-mail address: angelo.vaccari@unibo.it (A. Vaccari).

0920-5861/$ – see front matter © 2011 Elsevier B.V. All rights reserved.
doi:10.1016/j.cattod.2011.02.056

Table 1
Composition and surface characterisation data for fresh and spent catalysts.

Sample	Pt (wt.%)	Sn (wt.%)	BET surface area (in^2 g)	BJH pore volume (cm^3/g)	BJH pore width (Å)
Cat l fresh	1	–	138	0.432	91
Cat 2 fresh	1	1	135	0.419	90
Cnt 3 fresh	1	3	136	0.422	88
Cat l spent	1	–	128	0.389	94
Cat 2 spent	1	1	125	0.366	92
Cat 3 spent	1	3	126	0.372	93

successive incipient wetness impregnations. The γ-Al_2O_3 support (Al_2O_3–SCFa140 Sasol, BET surface area = 140 m^2/g) was at first impregnated by a solution of H_2PtCl_6 (Johnson Matthey) and dried under vacuum in rotavapor; then it was further heated at 110 °C for 2 h and calcined at 500 °C (10 °C/min) for 8 h. A second impregnation was performed using a solution of $SnCl_2{\cdot}H_2O$ (Alfa Aesar) in the appropriate amount for the desired Pt/Sn ratio, the product was dried in rotary evaporator, then heated at 110 °C for 2 h and calcined at 500 °C (10 °C/min) for 8 h.

2.2. Catalyst characterisation

Specific surface area determinations were performed in a Micromeritics ASAP 2020 instrument. The samples were previously outgassed at 120 °C until a pressure of 0.04 bar was reached and maintained for 30 min. Calcined solids were heated at 150 °C until 0.04 bar was reached, then kept 30 min at this temperature and finally heated up to 250 °C and maintained for 30 min. X-ray diffraction powder (XRDP) patterns were recorded on a Philips PW 1050/81 goniometer, equipped with a PW 1710 unit, using Cu-Kα radiation (λ = 0.15418 nm, 40 kW, 25 mA). Raman analysis were performed using a Renishaw 1000 instrument equipped with a Leica DMLM microscope, laser source Diod (780 nm) on both fresh and spent samples, in the last case the samples were pretreated under vacuum at 350 °C into desorb surrogate molecule adsorbed. Thermal-programmed-oxidation (TPO) and reduction (TPR) characterisations were performed using a Thermoquest TPDRO1100 instrument. The fresh and spent samples were loaded in a quartz reactor and pre-treated in nitrogen at 150 °C for 30 min to eliminate weakly adsorbed species. After cooling at room temperature, N_2 was replaced by the analysing gas (5% H_2 in argon for TPR tests, 5% O_2 in He for TPO), and the temperature was increased up to 500 °C (10 °C/min) for H_2-TPR and up to 600 °C (10 °C/min) for O_2-TPO and maintained for 20 min.

2.3. Catalytic activity tests

Catalytic tests were performed in a continuous tubular steel reactor (length 530 mm; internal diameter 8 mm) placed in a programmable furnace. Catalytic bed temperature was controlled by a thermocouple sliding internally. 3 cm^3 of catalyst (14/20 mesh) were loaded in the reactor and activated at 350 °C for 2 h under a 200 mL flow of H_2/N_2 (40/60, v/v). Liquid reactants (JetA1 surrogate or JA1-S) were vaporised before mixing with preheated diluent N_2, if applied. The JA1-S blend used in the present tests includes five components in the following volume percentages: dodecane 65%; methyl-cyclohexane 14%; ter-butylbenzene 10%; decalin 6%; tetralin 5%; 50 ppm of sulfur (when used) were introduced feeding 3-methylthiophen (all reactants were from Aldrich, purity grade >98%, and used without any further purification). Tests were performed in the 350–550 °C range, varying the feed composition from 10 to 100% of JA1-S in N_2: Finally also pure JA1-S containing 50 ppm of S was fed. The contact time and pressure were 2 s and 0.5 MPa in all tests. Effluent gases were analysed on-line by a Agilent 7890A gas-chromatograph equipped with a TCD, while the liquid products were analysed off line by the same GC using a FID detector.

3. Results and discussion

3.1. Catalyst characterization

Fig. 1A and B shows the XRDP patterns for Cat1-3, fresh and spent catalysts, i.e. samples downloaded after reaction in the following conditions: T = 450 °C; feed composition (93% surrogate–7% H2); contac time = 2 s; P = 0.5 MPa; time on stream = 5 h. All the fresh catalysts (Fig. 1A) show the presence of traces of crystalline Pt^0 cubic phase on the support (mixture of γ and δ-Al_2O_3), while the Sn-containing samples (Cat2 and Cat3) also provide evidence for the presence of traces of various alloys of Pt and Sn, in particular a Pt-rich alloy, Pt_9Sn-like. According to Lieske and Völter [20], the formation of Pt–Sn alloys on γ-Al_2O_3 depends on the Sn-concentration, because the metallic Pt catalyses the reduction of Sn(II) to Sn(0) and stabilises it as an alloy.

The catalysts after reaction (Fig. 1B) show a significant evolution of the active phase, depending on the Sn-content. Exposure to a reducing atmosphere, at relatively high pressure and temperature, leads to the further formation of Sn^0, which is stabilised in different Pt/Sn alloys. In particular, while the spent Sn-free sample (Cat1) displays an XRDP pattern comparable to that of the fresh sample, significant differences are visible on increasing the Sn-content. The spent sample containing the higher Sn-amount (Cat3) shows the further formation of Sn-rich alloys, probably hexagonal Pt–Sn- and/or cubic Sn–Pt_3-like alloys. The formation of these phases causes the decrease of peak intensities relative to Pt^0. For all samples a little amount of crystalline graphite is also detectable, formed during the reaction tests.

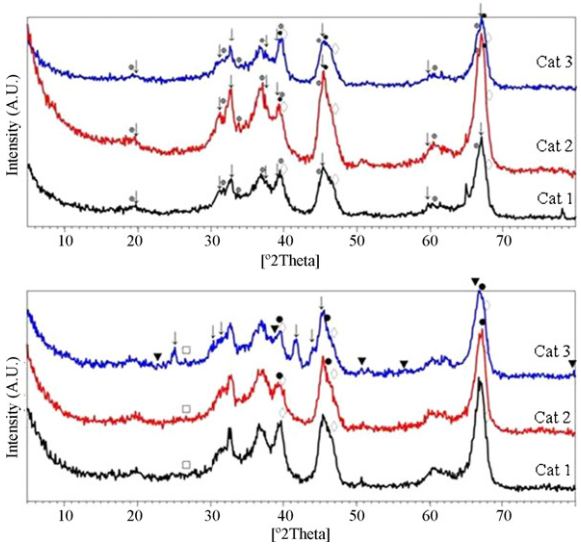

Fig. 1. (A) XRD powder patterns for fresh catalysts; phase identification: γ-Al_2O_3 00-050-0741 (●); δ-Al_2O_3 00-046-1131 (↓); Pt 00-001-1190 (◊); Pt_9Sn 03-065-9538 (●). (B) XRD powder patterns for spent catalysts; phase identification: graphite (□); Pt 00-001-1190 (◊); Pt_9Sn 03-065-9538 (●); $SnPt_3$ 00-035-1360 (▼); PtSn 01-089-2056 (↓).

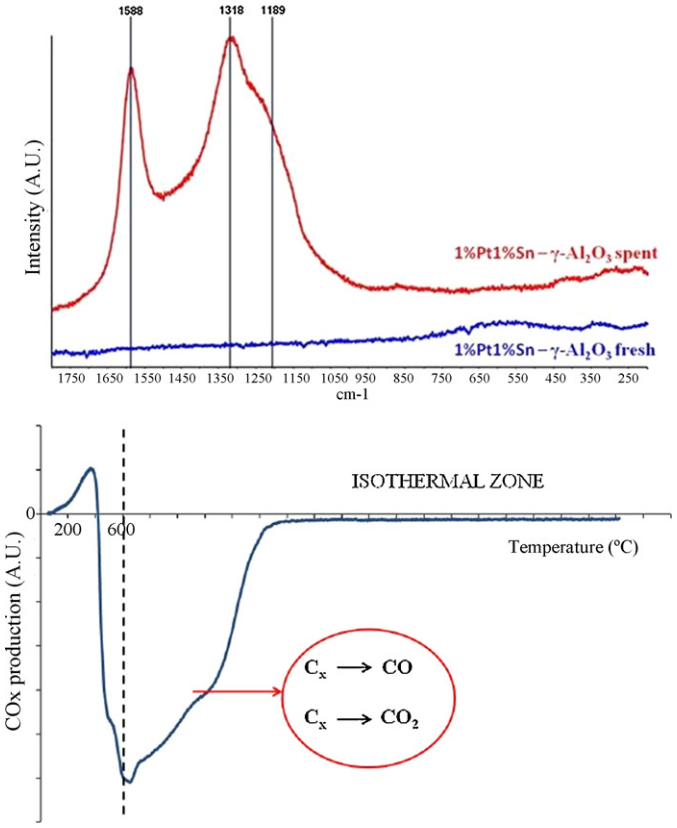

Fig. 2. (A) Raman spectrum of Cat2 fresh and spent, respectively. (B) TPO of spent Cat2 (C_x = surface tar).

The surface area for fresh samples (Table 1) is about 135 m^2/g and volume and pore diameter are similar for samples (about 0.420 mL and 90 Å, respectively), indicating that the different Sn-content does not affect the surface properties. The catalysts after reaction show a slight decrease (10% ca) of surface area and pore volume, mainly due to coke deposition. The presence of coke on the catalyst surface is confirmed by Raman spectra (Fig. 2A) that show two broad bands centered at 1588 and 1320 cm^{-1}, attributable to crystalline and disordered graphite [21], respectively. The TPO thermograms show for all samples (Fig. 2B) two negative peaks at about 500 and 600 °C, due to the combustion of adsorbed coke, suggesting that the catalysts may be easy regenerated by calcination. The H_2-TPR thermograms for fresh Cat1 and Cat3 (Fig. 3) show for the former catalyst, containing only Pt as active phase, the presence

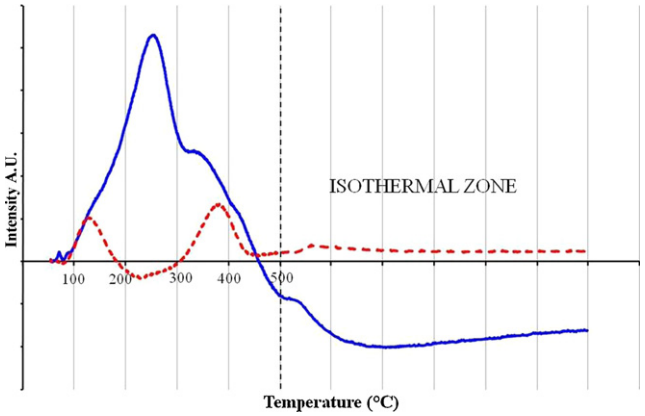

Fig. 3. TPR of fresh Cat1 (dot line) and Cat3 (full line).

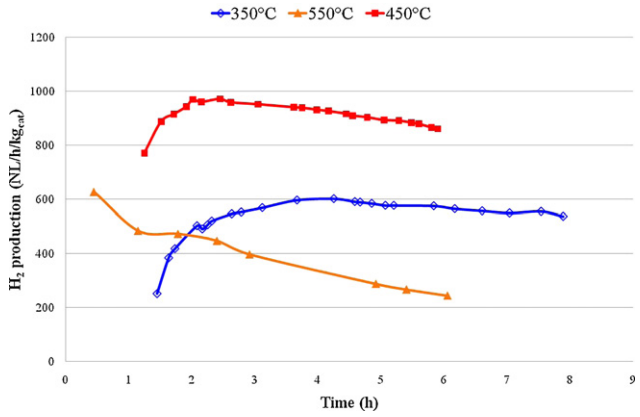

Fig. 4. H_2 productivity versus time at different temperatures for Cat2: 350 °C (◊); 450 °C (■); 550 °C (▲) (reaction conditions: 0.5 MPa; JetA1 surrogate (JA1-S): N_2 = 10:90 (v/v); contact time = 2 s).

of two peaks, the first one attributable to the reduction of surface Pt^{IV} to Pt^0 and the second, at higher temperature, probably due to a core and shell effect [20,22] or a strong interaction of the Pt with the support [23,24]. The addition of Sn significantly modify the reduction profile; Cat3 show a shoulder at low temperature again attributable to Pt^{IV} reduction, with further three peaks at higher temperatures. The most intense first peak may be attributed to the presence Pt-containing species easier reducible in presence of Sn, the second to the reduction of Pt/Sn alloys (also evidenced by XRD analysis) [20,25,26] and, finally, the peak at higher temperature to the reduction of surface SnO_2 to Sn^{II} or to Sn^0 [26].

3.2. Catalytic tests

Preliminary tests were performed on Cat2 (Pt/Sn = 1:1, w/w) to define the optimum temperature to maximize the H_2 production (Fig. 4), feeding a 10% (v/v) mixture of vaporised JA1-S diluted in N_2. The activity strongly increases with the temperature up to 450 °C, while a further increase of temperature quickly decreases the H_2 production, with a relevant catalyst deactivation. This behaviour may be correlated to the promotion by the high temperatures of side reactions, such as cracking and isomerisation, followed by catalyst surface coverage by coke. Thus, 450 °C may be considered a best compromise temperature for the reaction in terms of catalyst stability and H_2 productivity; thus subsequent tests were performed at this temperature.

H_2 for PEM fuel cells has to be very pure (~99.99%) and separation of H_2 from nitrogen may be not simple; moreover, to reach a defined amount of H_2, the volume of reactant fed to the reactor should be high, and thus, concentrated JA1-S feed appears most suitable. Fig. 5 shows the results of tests performed at 450 °C, feeding diluted and concentrated JA1-S. It is noteworthy that on increasing the feed concentration the H_2 production increases by a factor 3–4, although the catalyst life with time-on-stream slightly decreases. Thus these results indicate that it is possible to work with pure JA1-S and obtaining encouraging H_2 productivity per L of reactor.

The role of the active phase composition was investigated in reactions at 450 °C, feeding pure JA1-S to examinate the role of Sn in modulating the activity of Pt (Fig. 6). The Cat1 (Pt/Al_2O_3) catalyst has a high initial conversion, but deactivates quickly after few hours of time-on-stream, with a low overall H_2 production. The addition of Sn produces significant increases of catalyst activity and stability; however, while of the deactivation rate is enhanced by increasing the Sn-content (Cat3), the activity worsens moving from 1 wt.% of Sn (Cat2) to 3 wt.% (Cat3). The conversion values for the different

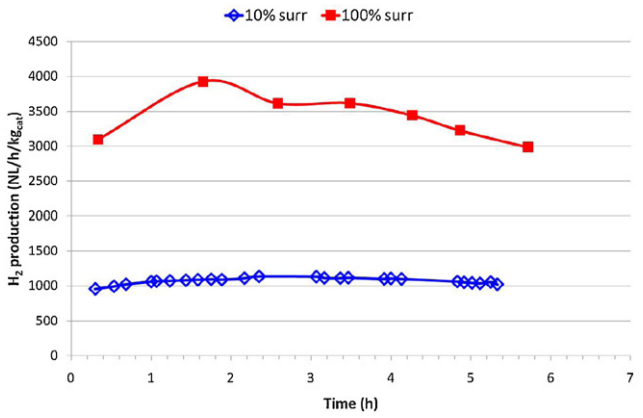

Fig. 5. H_2 productivity versus time for Cat2 feeding pure (■) or N_2 diluted (◊) JA1-S (reaction conditions: 0.5 MPa, 450 °C, contact time = 2 s).

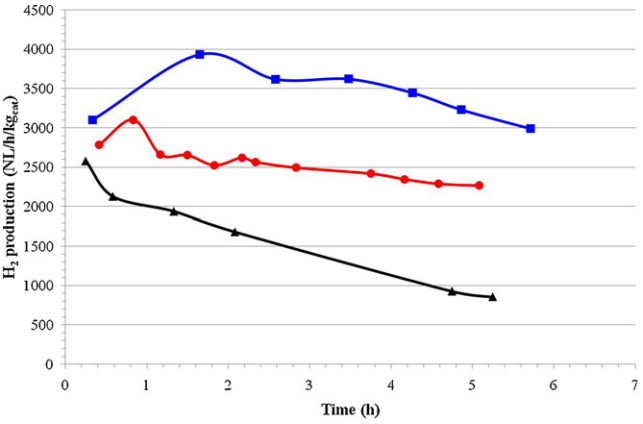

Fig. 6. H_2 productivity versus time for Cat1 (▲), Cat2 (■) and Cat3 (●) (reaction conditions: 0.5 MPa; 100% JAI-S; 450 °C, contact time = 2 s).

components of JA1-S (Fig. 7) reflect the H_2 productivity, showing higher reactivities for the cyclic compounds (methylcyclohexane, decalin and tetralin), while ter-butylbenzene almost does not react regardless of reaction conditions and catalyst compositions.

On the basis of these results, Cat2 seems to be the best compromise between H_2 productivity and stability with time-on-stream. Although the specific application does not require very long catalyst-life time, nevertheless first results show a good stability for some hundreds hours with, furthermore, the possibility to regenerate catalyst. Anyway in this preliminary work, the attention was

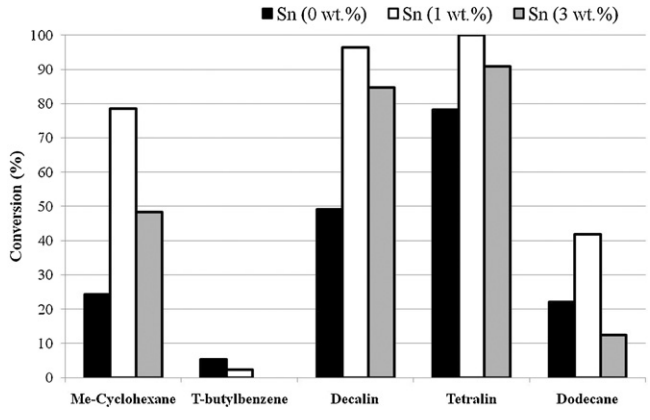

Fig. 7. Conversion values for the different components of JA1-S as a function of the Sn content (reaction conditions 0.5 MPa, 100% JA1-S, 450 °C; contact time = 2 s).

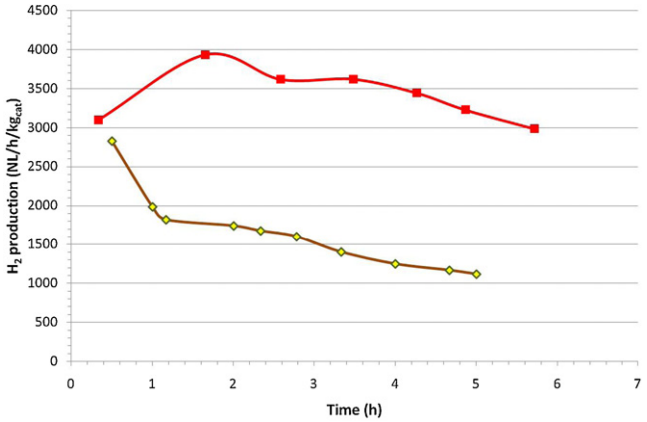

Fig. 8. H2 productivity versus time for Cat2 feeding S-free or 50 ppm of S JA1-S (reaction conditions: 0.5 MPa; 100% JA1-S; 450 °C; contact time = 2 s).

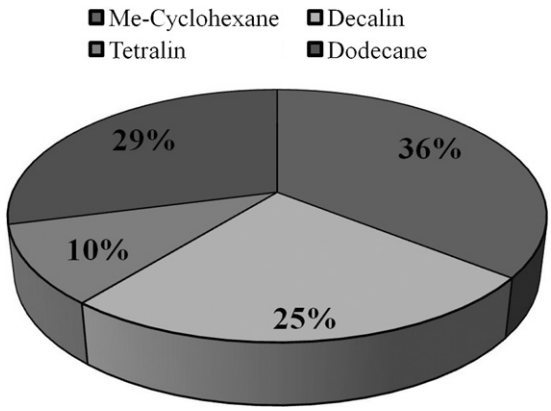

Fig. 9. Hydrogen productivity distribution as a function of the component present in the JA1-S (reaction conditions: Cat2; 0.5 MPa; 100% JA1-S; 450 °C; contact time = 2 s).

mainly focused on the role of reaction parameters and active phase composition on catalytic activity in order to verify the feasibility of the project. Its thio-tollerance was also investigated, considering that jet-fuels normally contain significant amounts of S-containing compounds, that may affect the activity of Pt. Fig. 8 provides a comparison between tests performed feeding JA1-S with and without 50 ppm of sulfur. The results show a significant and rapid deactivation in presence of S, probably due to the formation of platinum sulfide [27]. Thus, these Pt-containing catalysts may be applied using sulfur-free jet fuel, already available on the market, or require further improvement to increase their thiotolerance.

4. Conclusions

Very encouraging H_2 productivity values may be obtained in the partial dehydrogenation (PDh) of hydrocarbon blends, simulating jet fuel compositions, using a (1:1, w/w) Pt–Sn/alumina catalyst (Cat2) operating at 450 °C and feeding the sulfur-free surrogate Jet A1 fuel. Although at this temperature the catalyst deactivation is somewhat faster, it represents a good compromise between activity and deactivation rate. The presence of Sn tailors the reactivity of Pt by the formation of different Pt–Sn alloys, increasing the activity and reducing the undesired side reactions. The composition and reactivity of these alloys depend on the Sn-content; however, all these catalysts deactivate significantly in presence of S-contents lower than those present in the currently employed jet fuels. Cat2 shows a H_2 productivity of about 3000 $NL/kg_{cat}/h$, which is sufficient to produce 3 kW of electric power, considering purification steps and a fuel cell efficiency of 50%; this result is encouraging for

real applications on automotive or aviation transports. On the basis of JetA1-S composition and catalytic data it is possible to calculate the contribution of the different compounds to this H_2 productivity value (Fig. 9).

Acknowledgments

Financial support by the EU – FP7 for the GreenAir project (FP7-AAT-2008-RTD-1) – Grant Agreement No. 233862 – is gratefully acknowledged.

References

[1] S.G. Chalk, J.F. Miller, J. Power Sources 159 (2006) 73–80.
[2] S. Satyapal, J. Petrovic, C. Read, G. Thomas, G. Ordaz, Catal. Today 120 (2007) 246–256.
[3] H.L. Hellman, R. van den Hoed, Int. J. Hydrogen Energy 32 (2007) 305–315.
[4] R.B. Biniwale, S. Rayalu, S. Devotta, M. Ichikawa, Int. J. Hydrogen Energy 33 (2008) 360–365.
[5] C.L. Aardahl, S.D. Rassat, Int. J. Hydrogen Energy 34 (2009) 6676–6683.
[6] Y. Okada, E. Sasaki, E. Watanabe, S. Hyodo, H. Nishijima, Int. J. Hydrogen Energy 31 (2006) 1348–1356.
[7] Y. Saito, K. Aramaki, S. Hodoshima, M. Saito, A. Shono, J. Kuwano, K. Otake, Chem. Eng. Sci. 63 (2008) 4935–4941.
[8] M.P. Lazaro, E. Garcia-Bordejé, D. Sebastian, M.J. Lazaro, R. Moliner, Catal. Today 138 (2008) 203–209.
[9] M.R. Rahimpour, Int. J. Hydrogen Energy 34 (2009) 2235–2251.
[10] B. Wang, G.F. Froment, D. Wayne Goodman, J. Catal. 253 (2008) 239–243.
[11] N. Kariya, A. Fukuoka, T. Utagawa, M. Sakuramoto, Y. Goto, M. Ichikawa, Appl. Catal. A 247 (2003) 247–259.
[12] S. Hodoshima, N. Hiroaki, S. Yasukazu, Appl. Catal. A 292 (2005) 90–96.
[13] R.B. Biniwale, N. Kariya, M. Ichikawa, Catal. Lett. 105 (2005) 83–87.
[14] Y. Wang, N. Shah, F.E. Huggins, G.P. Huffman, Energy & Fuels 20 (2006) 2612–2615.
[15] S. Yolcular, O. Olgun, Catal. Today 138 (2008) 198–202.
[16] D. Sebastian, E.G. Bordejé, L. Calvillo, M.J. Lazaro, R. Moliner, Int. J. Hydrogen Energy 33 (2008) 1329–1334.
[17] K. Akamatsu, Y. Ohta, T. Sugawara, T. Hattori, S. Nakao, Ind. Eng. Chem. Res. 47 (2008) 9842–9847.
[18] P. Dung Tien, T. Satoh, M. Miura, M. Nomura, Fuel Process. Technol. 89 (2008) 415–418.
[19] P. Li, Y. Huang, D. Chen, J. Zhu, T. Zhao, X. Zhou, Catal. Commun. 10 (2009) 815–818.
[20] H. Lieske, J. Völter, J. Catal. 90 (1984) 96–105.
[21] F. Tuinstra, J.L. Koenig, J. Chem. Phys. 53 (3) (1970) 1126–1130.
[22] J.M. Badano, M. Quiroga, C. Betti, C. Vera, S. Canavese, F. Colma-Pascual, Catal. Lett. 137 (1–2) (2010) 35–44.
[23] H. Lieske, G. Lietz, H. Spindler, J. Voelter, J. Catal. 81 (8) (1983).
[24] T. Huizinga, J. van Grondelle, R. Prins, Appl. Catal. 10 (1984) 199–213.
[25] S.A. Bocanegra, S.R. de Miguel, I. Borbath, J.L. Margitflavi, O.A. Scleza, J. Mol. Catal. A 301 (2009) 52–60.
[26] A.D. Ballarini, P. Zgolicz, I.M.J. Vilella, S.R. de Miguel, A.A. Castro, O.A. Scleza, Appl. Catal. 381 (1–2) (2010) 83–91.
[27] S. Albertazzi, G. Busca, E. Finocchio, R. Glöckler, A. Vaccari, J. Catal. 223 (2004) 372–381.